J Neuropathol Exp Neurol

Vol. 69, No. 7
July 2010
pp. 717–728

ORIGINAL ARTICLE

Stem Cell Quiescence in the Hippocampal Neurogenic Niche Is Associated With Elevated Transforming Growth Factor-β Signaling in an Animal Model of Huntington Disease

Mahesh Kandasamy, Sebastien Couillard-Despres, PhD, Kerstin A. Raber, PhD, Michael Stephan, MD, Bernadette Lehner, Beate Winner, MD, Zacharias Kohl, MD, Francisco J. Rivera, PhD, Huu Phuc Nguyen, MD, Olaf Riess, MD, Ulrich Bogdahn, MD, Jürgen Winkler, MD, Stephan von Hörsten, MD, and Ludwig Aigner, PhD

Abstract

Cellular proliferation, differentiation, integration, and survival within the adult neural stem cell niche are altered under pathological conditions, but the molecular cues regulating the biology of this niche are mostly unknown. We examined the hippocampal neural stem cell niche in a transgenic rat model of Huntington disease. In this model, progressive cognitive deficits develop at the age of 9 months, suggesting possible hippocampal dysfunction. We found a disease-associated progressive decline in hippocampal progenitor cell proliferation accompanied by an expansion of the pool of 5-bromo-2-deoxyuridine label–retaining Sox-2–positive quiescent stem cells in the transgenic animals. Increments in quiescent stem cells occurred at the expense of cAMP-responsive element-binding protein–mediated neuronal differentiation and survival. Because elevated levels of transforming growth factor-β1 (TGF-β1) impair neural progenitor proliferation, we investigated hippocampal TGF-β signaling and determined that TGF-β1 induces the neural progenitors to exit the cell cycle. Although phospho-Smad2, an effector of TGF-β signaling, is normally absent in subgranular stem cells, it accumulated progressively in Sox2/glial fibrillary acidic protein–expressing cells of the subgranular zone in the transgenic rats. These results indicate that alterations in neurogenesis in transgenic Huntington disease rats occur in successive phases that are associated with increasing TGF-β signaling. Thus, TGF-β1 signaling seems to be a crucial modulator of neurogenesis in Huntington disease and may represent a target for future therapy.

Key Words: Adult neurogenesis, Huntington disease, Neural stem cells, Neuronal differentiation, Proliferation, Transforming growth factor-β.

INTRODUCTION

Huntington disease (HD) is a devastating neurodegenerative disease caused by a CAG trinucleotide repeat expansion within the huntingtin (*HD/IT15*) gene (1). Several transgenic animal models for HD have been established, and among the most widely used ones are the transgenic R6/1 and R6/2 mouse lines that express a transgene representing the exon 1 of the human HD gene bearing 115–157 CAG repeats (2). These transgenic mice develop severe neurological signs with an early onset and die within the first 2 to 4 months of life. Therefore, this model has only limited value for modeling a long-lasting and progressive neurological and neurodegenerative disorder such as HD.

To establish a more faithful HD model, we recently developed a transgenic model of HD in rats (tgHD) that carries a truncated huntingtin cDNA fragment encoding for 51 CAG repeats under the control of the rat huntingtin promoter (3). The tgHD rats exhibit an adult-onset neurological phenotype characterized by elevated anxiety, cognitive impairment, and slowly progressive motor dysfunction. These behavioral manifestations are accompanied by typical histopathologic alterations, such as neuronal nuclear inclusions in the basal ganglia and the hippocampus (3–5). The tgHD rats also have brain mitochondrial dysfunction and degeneration of medium spiny neurons (6, 7). In addition to behavioral and morphological abnormalities, tgHD rats have increased mortality starting at about 15 months of age (3). This slowly evolving disease thus reflects human HD more faithfully and permits a detailed analysis of progressive alterations in brain function and pathogenesis. Moreover, it provides a window of opportunity to scrutinize the impact of endogenous or

From the Institute of Molecular Regenerative Medicine (MK, SC-D, FJR, LA), Paracelsus Medical University, Salzburg, Austria; Department of Neurology (MK, SC-D, BL, BW, FJR, UB), University of Regensburg, University Hospital Regensburg; Institute of Functional and Applied Anatomy (KAR, MS, SVH), Hannover Medical School, Hannover; Experimental Therapy (KAR, SVH), Friedrich-Alexander-University Erlangen-Nürnberg, Erlangen; and Clinic of Psychosomatics and Psychotherapy (MS), Hannover Medical School, Hannover, Germany; The Salk Institute for Biological Studies (BW), Laboratory of Genetics, La Jolla, California; and Division of Molecular Neurology (ZK, JW), University Hospital Erlangen, Erlangen; and Department of Medical Genetics (HPN, OR), University of Tübingen, Tübingen, Germany.

SVH and LA contributed equally.

Send correspondence and reprint requests to: Ludwig Aigner, PhD, Institute of Molecular Regenerative Medicine, Paracelsus Medical University, Strubergasse 21, 5020 Salzburg, Austria; E-mail: ludwig.aigner@pmu.ac.at

This work was supported by Bayerische Forschungsstiftung, Munich, Germany (Francisco Rivera, Mahesh Kandasamy); by the Alexander von Humboldt Foundation (Beate Winner)–Georg Forster Program (Francisco Rivera); by the Bavarian State Ministry of Sciences, Research and the Arts (ForNeuroCell grant) (Sebastien Couillard-Despres, Beate Winner, Ulrich Bogdahn, Jürgen Winkler, Ludwig Aigner); by Regenion GmbH; by the Adalbert Raps Foundation (Jürgen Winkler); by the German Federal Ministry of Education and Research (BMBF grant no. 0312134, grant no. 01GG0706, grant no. 01G0979 and grant no. 01GN0505); and by EU-FP6-project DiMI, LSHB-CT-2005-512146.

induced cellular plasticity and/or restorative processes during the disease course (3).

The potential for adult rodent and human brains to generate new neurons from endogenous stem and progenitor cells is highly attractive in the field of regenerative medicine and is currently intensively investigated (8). We and others have previously reported that hippocampal progenitor cell proliferation and survival are impaired in the R6/1 and R6/2 tgHD models (9–14). The sequence of cellular events and molecular mechanisms that compromise neurogenesis in HD animal models are not understood.

The expression of the pleiotropic cytokine transforming growth factor-β1 (TGF-β1) and TGF-β signaling components are elevated in the degenerating HD brain (6, 15–17). Elevation of cerebral TGF-β1 levels not only inhibits progenitor proliferation in the adult hippocampus (18, 19) but also impairs hippocampus-dependent learning (20–24). The tgHD rats develop cognitive deficits (3–5), and they develop dilation of the lateral ventricles beginning at the age of 8 months (3); the latter process might also be mediated via TGF-β1 (24–27). These data raise the possibility that TGF-β1 is involved in the stem cell niche remodeling observed in numerous neurodegenerative diseases such as HD.

In the present study, we investigated hippocampal neurogenesis in transgenic HD models and a possible correlation between the observed neurogenic modulations and alterations in TGF-β signaling. We analyzed 2 age cohorts of tgHD rats: 8-month-old rats, shortly before cognitive deficits can be detected, and 12-month-old rats, the age at which they exhibit the most cognitive dysfunction. This report focuses mainly on the tgHD rat model, but we also document similar alterations in R6/2 HD mice and in rats given direct intracerebroventricular infusions of TGF-β1 protein.

MATERIALS AND METHODS

Animals

Eight- and 12-month-old male rats were obtained from a colony of tgHD and wild-type (WT) littermates established at the central animal facility of the University of Hannover, Hannover, Germany (3). Offspring derived from generation F10 were used. The presence of the huntingtin transgene in the tgHD rats was confirmed by tail-DNA genotyping at the age of 3 weeks. Tissues from R6/2 mice (12) and from TGF-β–infused rats (19) were also used. All experiments were carried out in accordance with the European Communities Council Directive of November 24, 1986 (86/609/EEC), and were approved by the local governmental commission for animal health.

BrdU Labeling

Labeling of dividing cells was performed by intraperitoneal injection of the thymidine analogue 5-bromo-2-deoxyuridine ([BrdU] Sigma, Steinheim, Germany) at 50 mg/kg of body weight using a sterile solution of 10 mg/mL of BrdU dissolved in a 0.9% (wt/vol) NaCl solution. For the proliferation experiment, rats received 2 BrdU injections with an interval of 12 hours and were killed 24 hours after the second BrdU pulse (8 months: WT, n = 4; tgHD, n = 8; 12 months: WT, n = 4; tgHD, n = 8). For the cell survival experiments, BrdU injections were performed daily on 5 consecutive days, and the rats were killed at day 30. Group sizes were the same in both experiments.

Tissue Processing and Immunostaining

Rats were deeply anesthetized using a ketamine (20.38 mg/mL), xylazine (5.38 mg/mL), and acepromazine (0.29 mg/mL) mixture. Transcardial perfusion was performed with 0.9% (wt/vol) NaCl solution followed by 4% paraformaldehyde, 0.1 mol/L sodium phosphate solution (pH 7.4). Brains were removed and postfixed in paraformaldehyde overnight at 4°C. Tissue was then cryoprotected in 30% (wt/vol) sucrose, 0.1 mol/L sodium phosphate solution (pH 7.4). Brains were cut into 40-μm sagittal sections using a sliding microtome on dry ice. Sections were stored at −20°C in cryoprotectant solution (ethylene glycol, glycerol, 0.1 mol/L phosphate buffer, pH 7.4, 1:1:2 by volume). Free-floating sections were treated with 0.6% H_2O_2 in Tris-buffered saline ([TBS] 0.15 mol/L NaCl, 0.1 mol/L Tris-HCl, pH 7.5) for 30 minutes. For detection of the incorporated BrdU by immunohistochemistry (IHC), pretreatment of tissues was performed as previously described (28). After extensive washes in TBS, sections were blocked with a solution composed of TBS, 0.1% Triton X-100, 1% bovine serum albumin, and 0.2% teleostean gelatin (Sigma, Taufkirchen, Germany) for 1 hour. This buffer was also used during the incubation with antibodies. Primary antibodies were applied overnight at 4°C. The sections were washed extensively and further incubated with biotin-conjugated species-specific secondary antibodies followed by a peroxidase-avidin complex solution (Vectastain Elite ABC kit; Vector Laboratories, Burlingame, CA). The peroxidase activity of immune complexes was revealed with a solution of TBS containing 0.25 mg/mL 3, 3′-diaminobenzidine (Vector Laboratories), 0.01% (vol/vol) H_2O_2, and 0.04% (wt/vol) $NiCl_2$. Sections were placed on Superfrost Plus slides (Menzel, Braunschweig, Germany) and mounted on Neo-Mount (Merck, Darmstadt, Germany). For epifluorescence immunodetection, sections were washed extensively and incubated with fluorochrome-conjugated species-specific secondary antibodies overnight at 4°C. Sections were placed on slides and mounted on Prolong Antifade kit (Molecular Probes, Eugene, OR). Photodocumentation was done using a Leica microscope (Leica, Wetzlar, Germany) equipped with a Spot digital camera (Diagnostic Instrument Inc, Sterling Heights, MI), and epifluorescence observation was performed on a confocal scanning laser microscope (Leica TCS-NT; Leica Microsystems, Bensheim, Germany).

The following antibodies and final dilutions were used. Primary antibodies: rat anti-BrdU 1:500 (Oxford Biotechnology, Oxford, UK), mouse anti–proliferating cell nuclear antigen (PCNA) 1:500, goat anti-doublecortin ([DCX] C-18) 1:500 (both from Santa Cruz Biotechnology, Santa Cruz, CA), mouse anti-NeuN (neuronal nuclei) 1:500 (Chemicon, Temecula, CA), rabbit anti–glial fibrillary acidic protein (GFAP) 1:1000 (Dako, Glostrup, Denmark), guinea pig anti-GFAP 1:500 (Progen, Heidelberg, Germany), rabbit anti-pSmad2 (phospho-Smad2 [Ser465/467], Cell Signaling, Danvers, MA) 1:50 (Cell Signaling, Denver, CO), goat anti-Sox2 1:500 (Santa Cruz Biotechnology, Santa Cruz, CA). The

secondary antibodies: donkey anti-goat, -mouse, -rabbit, or -rat conjugated with Alexa 488 (1:1000; Molecular Probes), rhodamine X (Dianova, Hamburg, Germany), Cy5 or biotin 1:500 (Jackson Immuno Research, West Grove, PA).

Counting Procedures

All morphological analyses were performed blinded on coded slides. Every sixth section (240-μm interval) of 1 hemisphere was selected from each animal and processed for IHC. To analyze cell proliferation in the dentate gyrus (DG) (Experiment I), BrdU-positive and PCNA-positive cells were counted. To assess cell survival in DG (Experiment II), BrdU-positive cells were counted. To investigate neurogenesis, the numbers of neural precursor cells in every 12th section (480-μm interval) stained for DCX were determined. Cells stained for BrdU, PCNA, and DCX were counted with 400× magnification on a light microscope (Leica) and multiplied by 6, respectively, 12, to obtain an estimate of total immunopositive cell numbers. The reference volume was determined by tracing the granule cell layer (GCL) of the hippocampal DG using a semiautomatic stereology system (Stereoinvestigator; MicroBrightField, Colchester, VT).

Total numbers of DG neurons were determined by counting NeuN-positive cells in the GCL of the dorsal hippocampal DG in every 12th section (480-μm intervals). A systematic counting procedure, similar to the optical dissector described by Gundersen et al (29) and Williams and Rakic (30), was used. The NeuN-positive cells were counted within a 15 × 15-μm counting frame that was spaced in a 150 × 150-μm counting grid. The GCL nuclei intersecting the uppermost focal plane (exclusion plane) and those intersecting the exclusion boundaries of the counting frame were not counted. The sample volume of NeuN-positive cells was determined by multiplying the number of frames counted × size of the counting frame × thickness of the section. The volume of the entire structure was calculated by multiplying the reference volume with the number of sections. To obtain the neuronal density, the total number of cells counted was divided by the sample volume and represented as cells per microliter. The total number of neurons was calculated by multiplying the density with the entire DG volume. All extrapolations were calculated for 1 hippocampus and should be doubled to represent the total hippocampal values.

The BrdU-positive cells often appeared in clusters that can be considered as proliferating units (31). The sizes of the clusters (>3 cells) in square micrometers and numbers of BrdU-positive cells per cluster (proliferating units) were quantified on an Olympus microscope (Olympus, Hamburg, Germany) using analySIS 3.2 software (Soft Imaging Systems, Munster, Germany). For analysis of mitotic neuronal precursor cells, the BrdU-positive/DCX-positive cells were analyzed in BrdU-positive cell clusters 24 hours after BrdU injection.

To determine the frequency of neuronal differentiation and cell fate of newborn cells (Experiment II), a series of every sixth brain section (240-μm interval) was stained and analyzed for BrdU/NeuN/GFAP by triple immunofluorescence. Undifferentiated, self-renewing, and quiescent cells were identified by BrdU/Sox2/PCNA triple immunofluorescence. Signaling for TGF-β1 was identified by the presence of pSmad2 in GFAP-positive/Sox2-positive and in DCX-positive/NeuN-positive cells. Neuronal differentiation was analyzed by BrdU/NeuN double staining, and astroglial differentiation was identified by BrdU/GFAP double labeling. Confocal examination was performed using a Leica TCS-NT confocal laser microscope equipped with a 40× PL APO oil objective (1.25 numeric aperture) and a pinhole setting that corresponded to a focal plane of 2 μm or less. Because of the relatively high age of the animals with an overall low level of neurogenesis, every BrdU-positive cell was examined in the cell fate analysis. For determination of TGF-β1 signaling in neural stem cells, 50 Sox2 or Sox2/GFAP double-positive cells were examined for pSmad2 colocalization.

Western Blotting

Hippocampi from WT or HD rats (3 animals each) or neurospheres were lysed in buffer (0.7% NP40, 50 mmol/L Tris-HCl [pH 8.0], 0.1 mmol/L EDTA [pH 8.0], 250 mmol/L NaCl, 10% glycerol, 0.2 mmol/L Na_3VO_4, 1 mmol/L phenylmethylsulfonyl fluoride, 10 mmol/L dithiothreitol, 2 μg/mL aprotinin, and 1 μg/mL pepstatin) and centrifuged at 17,900 × *g* for 15 minutes at 4°C. The protein concentration was determined using BCA test (Sigma), and the resulting supernatants (20 μg of total protein) were size separated by 12% sodium dodecyl sulfate polyacrylamide gel electrophoresis and transferred onto nitrocellulose membranes (Schleicher and Schuell, Dassel, Germany) by the semidry electroblot method (Biometra Fast blot; Biometra Biomedizinische Analytik, Gottingen, Germany). To determine the endogenous level of TGF-β1 signaling in the rat hippocampi, the antibodies used for Western blot and their dilutions were rabbit anti-phosphoSmad2 (Ser465/467) 1:1000 and mouse anti-Smad2 1:1000 (both from Cell Signaling). The levels of cAMP-responsive element-binding protein (CREB) signaling were detected using rabbit anti–phospho CREB1 (Ser133) 1:1000, rabbit anti-CREB 1:1000 (both from Cell Signaling), and rabbit anti-actin 1:5000 (Sigma). Secondary antibodies were goat anti-mouse 1:5000 (Chemicon) or anti–rabbit immunoglobulin G horseradish peroxidase antibodies 1:10,000 (Dianova), and detection was performed using the ECL Plus chemiluminescence system and exposed to Hyperfilm (both from Amersham Pharmacia, Freiburg, Germany).

Intracerebroventricular Infusions of TGF-β1

Sixteen 2- to 3-month-old female Fischer-344 rats (mean weight, 180 g) were given intracerebroventricular infusions via stainless steel cannulas connected to osmotic minipumps (Model 2002, ALZET; Durect Corp, Cupertino, CA), as described (19). Rats received either recombinant TGF-β1 (500 ng/mL) dissolved in artificial cerebrospinal fluid (aCSF) or aCSF only (n = 8 each) at a flow rate of 0.5 μL/hour for 14 days. During the last 4 days of the pump period, the rats received daily intraperitoneal injections of 50 mg/kg BrdU and were then intracardially perfused with 4% paraformaldehyde.

Neural Progenitor Cultures

Adult hippocampal progenitor cells were isolated and cultured as described (32). Briefly, 2- to 4-month-old female

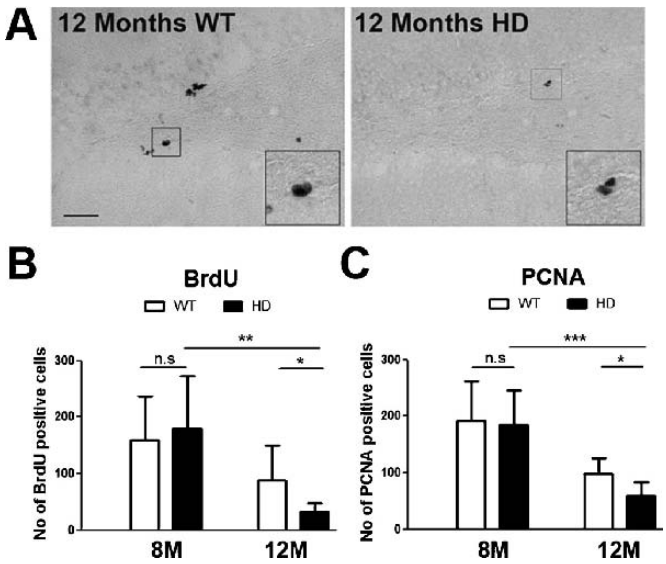

FIGURE 1. Impaired hippocampal proliferation in 12-month-old transgenic rat model of Huntington disease (tgHD). **(A)** Labeling of 12-month-old wild-type (WT) and tgHD hippocampi with 5-bromo-2-deoxyuridine (BrdU). Insets are higher magnifications of the selected fields. Scale bars = 100 μm. **(B, C)** Quantitative analysis of BrdU-positive cells in 8- and 12-month-old rats 24 hours after BrdU injection **(B)** and of proliferating cell nuclear antigen (PCNA)–positive cells **(C)** expressed as positive cells per hippocampus (mean ± SD). In 8-month-old rats, there was no difference between WT and tgHD. In 12-month-old tgHD rats, the numbers of BrdU-positive **(B)** and PCNA-positive (*$p < 0.05$) cells were reduced compared with WT. There were fewer BrdU-positive (**$p < 0.01$) and PCNA-positive (***$p < 0.001$) proliferating cells in the 12- versus 8-month-old tgHD animals. n = 4 for WT and n = 8 for tgHD. **(B, C)** $p < 0.05$; 2-way analysis of variance–Bonferroni posttest.

Fischer-344 rats (Charles River Deutschland GmbH, Germany) were decapitated, and the hippocampi were dissected. The tissue was homogenized, and cells were resuspended in neurobasal medium (Gibco BRL, Germany) containing B27 supplement (Gibco BRL), 2 mmol/L L-glutamine (PAN Biotech, Aidenbach, Germany), 100 U/mL penicillin/100 μg/mL streptomycin (PAN Biotech). For expansion, the NB/B27 was growth factor supplemented with 2 mg/mL heparin (Sigma), 20 ng/mL FGF-2 (R&D Systems, Wiesbaden, Germany), and 20 ng/mL epidermal growth factor (R&D Systems) (proliferation medium). The cell suspension from the hippocampi of 5 rats was seeded into a T25 flask (TPP, Zurich, Switzerland) in 5 mL of proliferation medium. The cultures were maintained at 37°C in a humidified incubator with 5% carbon dioxide, and half of the medium was changed every 3 to 4 days. For passaging, cells were dissociated using Accutase (PAA, Pasching, Austria), and a total of 5×10^5 cells were seeded in a T75 flask (TPP). Neurosphere cultures from passages 3 to 7 were used for the experiments.

Cell Cycle Analysis

The cell cycle was analyzed by fluorescence-activated cell sorting using a modified Ki67/PI staining protocol from Endl et al (33). Neural progenitors derived from adult rat hippocampus were seeded into T25 flasks (TPP) and stimulated with 10 ng/mL TGF-β1 or PBS control for 7 days. The TGF-β1 was added every second day. On Day 7, the cells were spun down, the medium was removed, and cells were fixed with 1 mL ice-cold 70% EtOH. After fixation, the cells were washed with ice-cold PBS and then resuspended in 500 μL ice-cold PBS containing 0.1% Triton X-100 and incubated for 5 minutes on ice. After 2 washing steps, the cells were resuspended in 100 μL of a 1:6 dilution of the antibodies in PBS (100 μL PBS + 20 μL antibody immunoglobulin G or Ki67; BD Biosciences, Pharmingen; fluorescein

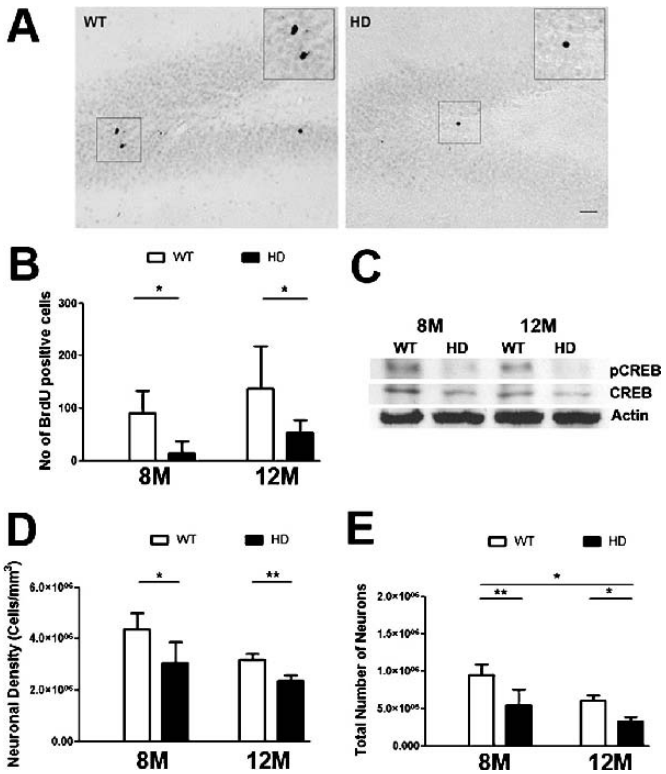

FIGURE 2. Reduced cell survival in a transgenic rat model of Huntington disease (tgHD) was associated with diminished cAMP-responsive element-binding protein (CREB) signaling. **(A)** Cells that were positive for 5-bromo-2-deoxyuridine (BrdU) in the dentate gyrus (DG) 4 weeks after injecting BrdU into 8-month-old wild-type (WT) and tgHD rats. Scale bars = 50 μm. Insets are higher magnifications of the selected fields. **(B)** Quantitative analysis of BrdU-positive cells demonstrates reduced numbers of labeled cells in the tgHD compared with WT DG at 8 months (*$p < 0.05$) and 12 months (*$p < 0.05$). **(C)** Western blot analysis demonstrates lower levels of CREB and pCREB in tgHD hippocampi. Actin was used as a loading control. **(D)** Quantitative analysis of NeuN-positive cell densities in the DG. There was a lower neuronal density in the tgHD rats versus WT at 8 months (*$p < 0.05$) and 12 months (**$p < 0.001$). **(E)** Quantitative analysis of total DG neuron numbers. There were fewer neurons in the tgHD versus WT rats at 8 months (**$p < 0.01$) and 12 months (*$p < 0.05$). For **(B)**, **(D)**, and **(E)**, data were expressed as mean ± SD; 2-way analysis of variance–Bonferroni posttest was performed; n = 4 for WT and n = 8 for tgHD.

isothiocyanate–conjugated antibodies). After 30 to 40 minutes of incubation at 4°C, the cells were washed with 1 mL PBS and then resuspended in PBS for staining. For PI staining, the cells were resuspended in 470 μL PBS. Cells without PI staining were resuspended in 495 μL. All samples were treated with 5 μL of RNase for 1 hour to eliminate the RNA that would interfere with the PI staining. After this 1-hour incubation at 37°C, 25 μL of PI was added to the respective samples. The stained cells were analyzed with the flow cytometer (FACS Calibur; Becton Dickinson, Heidelberg, Germany). Data were analyzed using Win MDI 2.8 software.

Statistical Analysis

The data were presented as mean values ± SD. Two-way analysis of variance (groups × age) and Bonferroni posttest was used for analyzing numbers of PCNA-positive and BrdU-positive cells, numbers of BrdU clusters, numbers of BrdU-positive cells per clusters, sizes of BrdU clusters, total DCX-positive cells, total neuronal number and neuronal density, and percentage of BrdU/NeuN/GFAP- and BrdU/Sox2/PCNA-positive cells. One-way analysis of variance test was used for percentage of Sox2/GFAP/pSmad2-positive cells, and a Tukey test comparison was performed for post hoc analysis. Student *t*-test was applied for analyzing the number of PCNA-positive cells in R6/2 mice, percentage of BrdU/DCX double-positive cells in tgHD and WT rats, numbers of BrdU-positive cells in the TGF-β infusion study, and for cell cycle–phase analysis. Statistical analysis was performed using Prism (Prism GraphPad Software, San Diego, CA). The significance level was at $p < 0.05$, unless otherwise indicated.

RESULTS

Cognitive impairment is a prominent manifestation in HD patients and in animal models of HD (4, 17, 34, 35). In

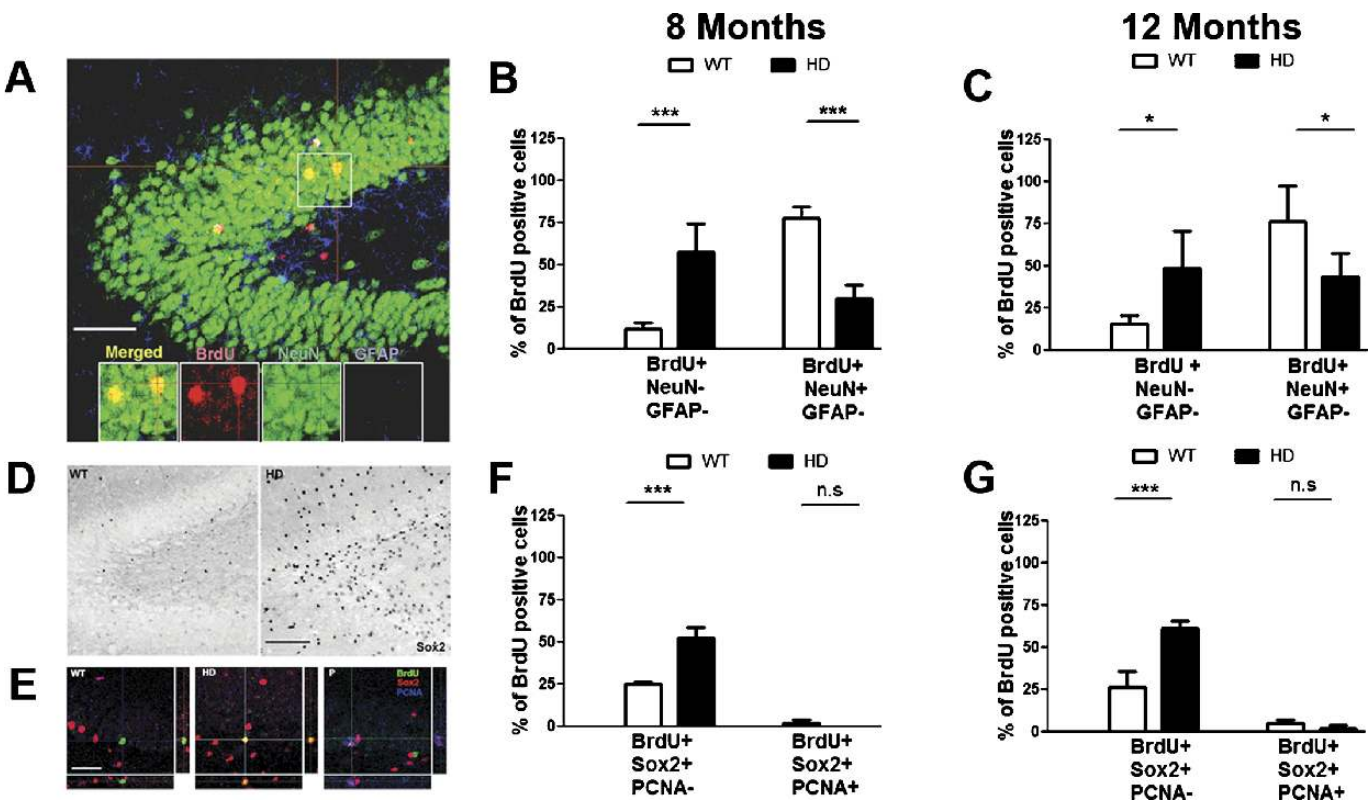

FIGURE 3. Deficiency in neuronal differentiation and augmentation of stem cell quiescence in a transgenic rat model of Huntington disease (tgHD). **(A)** Confocal analysis of 5-bromo-2-deoxyuridine (BrdU)–positive cells (red) that colocalize with NeuN (green) or with glial fibrillary acidic protein (GFAP) (blue) 4 weeks after BrdU injection of 8-month-old wild-type (WT) rats. Scale bars = 50 μm. **(B, C)** Quantitative analysis of BrdU-positive cells that did not colocalize with a differentiation marker or that colocalized with NeuN for neuronal differentiation in 8-month-old **(B)** and 12-month-old **(C)** rats. Reduction in neuronal differentiation was accompanied by an increase in numbers of undifferentiated cells (mean ± SD; ***$p < 0.0001$; *$p < 0.05$; 2-way analysis of variance–Bonferroni posttest). **(D)** Sox2 staining in the dentate gyrus (DG) of 12-month-old WT and tgHD rats. There was prominent immunoreactivity for Sox2 in the tgHD DG. Scale bars = 100 μm. **(E)** Triple staining of BrdU (green)/Sox2 (red)/proliferating cell nuclear antigen (PCNA) (blue) in 8-month-old WT and tgHD DG 4 weeks after BrdU injection. In WT DG, BrdU-positive cells were Sox2 and PCNA negative; in tgHD DG, BrdU-positive cells were Sox2 positive but PCNA negative. A control for PCNA (P) was included. Scale bars = 50 μm. **(F, G)** Quantitative analysis of BrdU-positive cells that were Sox2 positive but PCNA negative. The percentages of BrdU-positive Sox2-positive PCNA-negative cells were greater in tgHD than WT in 8-month-old (***$p < 0.0001$) **(F)** and 12-month-old (***$p < 0.0001$) rats **(G)**. There were no differences in BrdU-positive Sox2-positive PCNA-positive cells. n = 4 for WT and n = 8 for tgHD.

the tgHD rat model, working memory deficits start to develop within 9 months and reach a plateau at 12 months of age (4). Because working memory is tightly associated with hippocampal function and requires persisting neurogenesis, we hypothesized that the hippocampal stem cell niche in tgHD animals might undergo fundamental molecular and cellular changes affecting neurogenesis.

Hippocampal Cell Proliferation Was Decreased Between 8 and 12 Months of Age in tgHD Rats

The proliferation of neural progenitor cells in the DG of tgHD rats and WT littermates was analyzed by determining the numbers of BrdU-positive cells (Fig. 1A). At 8 months of age, tgHD rats showed a frequency of BrdU incorporation similar to their WT counterparts (WT, 159 ± 78 vs HD, 179 ± 93) (Fig. 1B). In contrast, in 12-month-old rats, the number of BrdU-labeled cells in the DG was significantly reduced compared with WT (WT, 88 ± 62 vs HD, 32 ± 15) (Figs. 1A, B). Analysis of PCNA, a protein expressed throughout the cell cycle, by IHC confirmed this significant reduction in proliferating cells in 12-month-old tgHD rats (WT, 99 ± 26 vs HD, 60 ± 24) (Fig. 1C). Inasmuch as aging is a potent inhibitor of neurogenesis, this may account for the more pronounced and significant decline in DG cell proliferation in the tgHD versus WT animals (Figs. 1B, C).

Impaired Survival of Newly Generated Cells Was Associated With Reduced CREB Signaling in tgHD Rat Hippocampus

Next, we analyzed the survival and fate of newly generated cells in the tgHD rats 4 weeks after BrdU labeling of proliferating cells (Fig. 2A). The total number of BrdU-positive cells was significantly lower in the DG of tgHD rats compared with WT at 8 months (WT, 91.5 ± 41 vs HD, 14.2 ± 23; Fig. 2B) and 12 months (WT, 137 ± 82 vs HD, 53 ± 25; Fig. 2B) of age, indicating that the survival of newly generated cells in the DG of tgHD rats was reduced than in WT littermates.

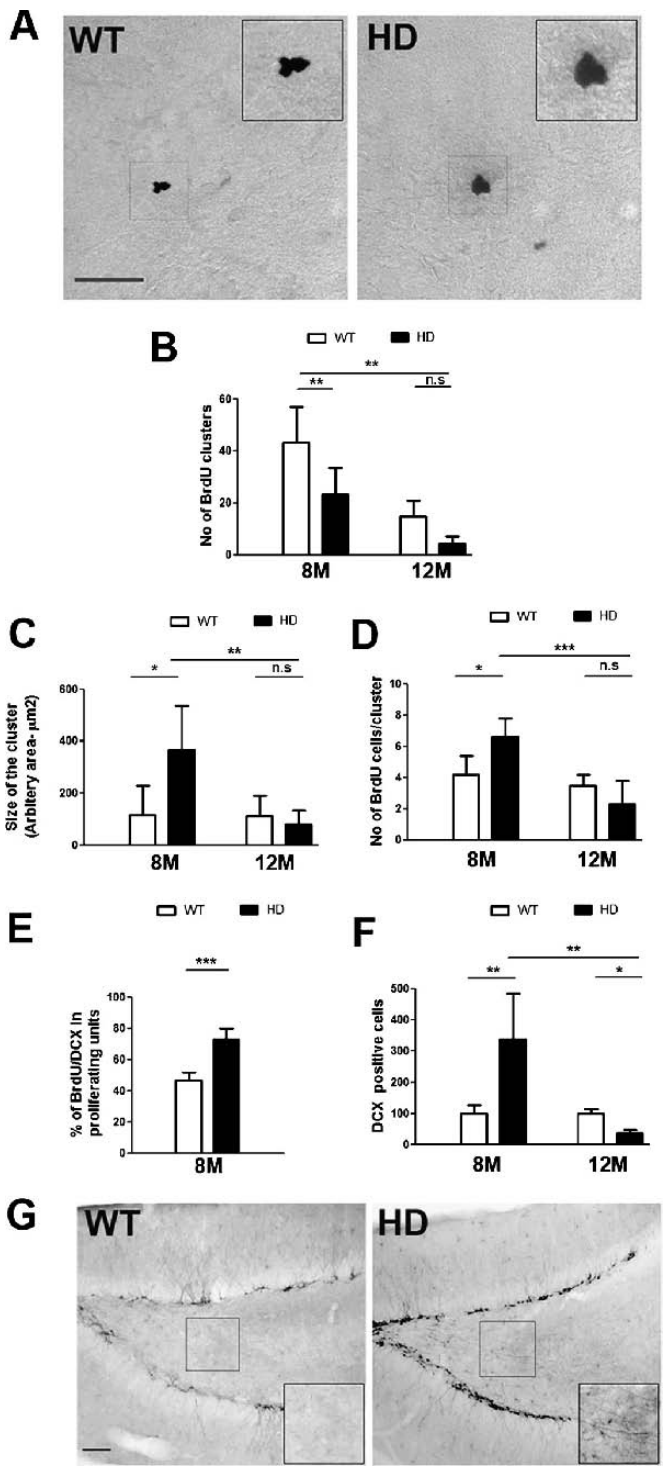

FIGURE 4. Neuroblast proliferation in 8-month-old transgenic rat model of Huntington disease (tgHD) hippocampus. **(A)** Clusters of 5-bromo-2-deoxyuridine (BrdU)–positive cells in 8-month-old wild-type (WT) and tgHD dentate gyrus (DG) 24 hours after BrdU injection. Scale bars = 50 μm. **(B–D)** Quantitative analysis of numbers of BrdU clusters **(B)**, size of BrdU clusters **(C)**, and number of BrdU-positive cells within a cluster **(D)**. Data were expressed as mean ± SD; 2-way analysis of variance–Bonferroni posttest. In tgHD DG, the numbers of proliferating units were less than those in WT DG (**$p < 0.001$), but the sizes of the clusters (*$p < 0.05$) and numbers of BrdU-positive cells within a cluster (*$p < 0.05$) were greater in 8-month-old tgHD than in WT rats. **(E)** Quantitative analysis of BrdU-positive cells in proliferating units that were double-cortin (DCX) positive for neuroblast proliferation in 8-month-old WT and tgHD DG 24 hours after BrdU injection. There were more BrdU-positive DCX-positive cells in the tgHD DG (***$p < 0.0001$). **(F)** Quantitative analysis of the percentages of DCX-positive cells in WT and tgHD DG in 8- and 12-month-old rats. The percentage of DCX-positive cells was greater in the 8-month-old tgHD DG (**$p < 0.001$); whereas in the DG of 12-month-old tgHD rats, the percentage of DCX-positive cells was less than those in WT DG (*$p < 0.05$). **(G)** Cells positive for DCX in 8-month-old WT and tgHD DG. Scale bars = 50 μm. Insets are higher magnifications of the selected hilar fields. In the tgHD DG, there were higher numbers of DCX-positive cells and DCX expression was greater in axons in the hilar region. **(B–F)** n = 4 for WT; n = 8 for tgHD.

Signaling via the CREB is known to be involved in regulating neuronal survival (36, 37). Thus, we hypothesized that the reduced survival of newly generated cells observed in tgHD rats might correlate with altered CREB signaling. Western blot analysis demonstrated reduced expression of CREB protein in the hippocampi of tgHD rats compared with WT (Fig. 2C). Moreover, the levels of CREB phosphorylation were diminished in tgHD rats (Fig. 2C).

The proliferation of neural progenitors and cell survival in tgHD rat brain might be determined by the demand on new neurons and thus influenced by the total number or density of existing DG neurons. To exclude the possibility that reduced neuronal survival was a consequence of an excess of DG neurons, we analyzed NeuN-positive neurons in the hippocampal DG. The number and density of NeuN-positive cells were significantly lower in the DG of tgHD versus WT rats at 8 and 12 months of age (Figs. 2D, E), suggesting that the reduced proliferation of progenitors in the DG is not a consequence of an excess of DG neurons.

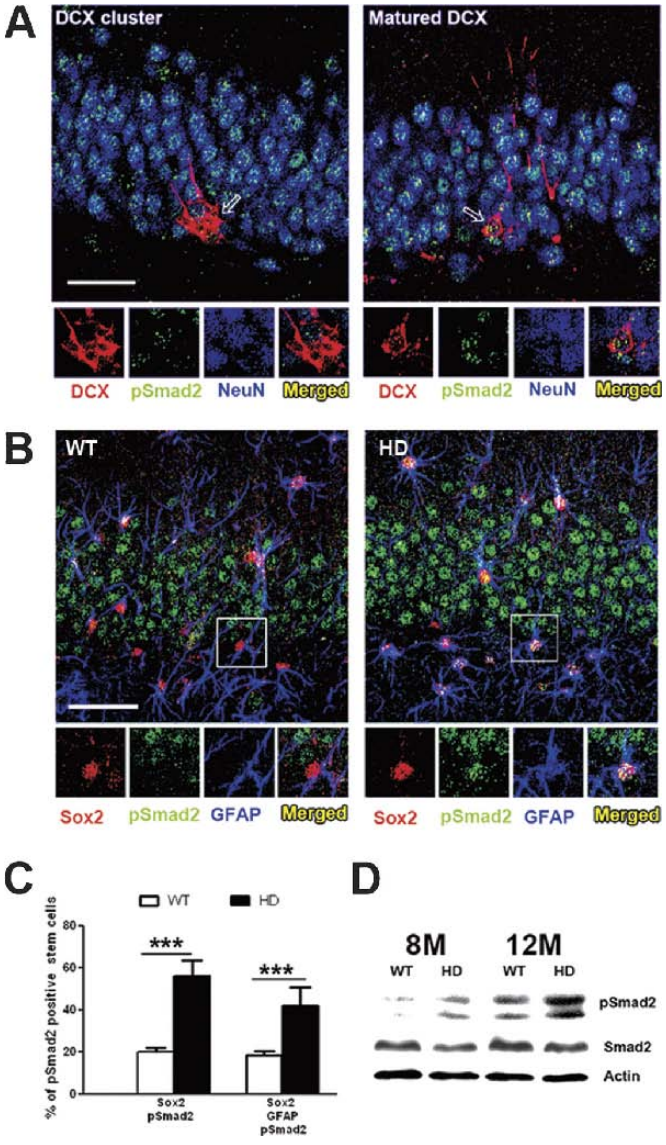

Increased Quiescence of Newly Generated Cells in tgHD DG

The neuronal and astroglial differentiation of newly generated cells was analyzed by confocal analysis of BrdU-positive cells that were NeuN positive (neurons) or GFAP positive (astroglia) 4 weeks after BrdU labeling (Fig. 3A). In the DG of 8- and 12-month-old WT rats, newly generated cells predominantly differentiated into neurons; whereas in tgHD rats, the neuronal differentiation was significantly reduced (8 months: WT, 77.7% ± 6.6% vs HD, 30.3% ± 7.9%; 12 months: WT, 76.5% ± 21% vs HD, 43.8% ± 13.6%) (Figs. 3B, C). Regardless of the age and the presence of the transgene, approximately 10% of newly generated cells differentiated into GFAP-positive astroglial cells (data not shown). There was, however, a striking increase in the pool of BrdU-positive cells that were neither NeuN positive nor GFAP positive in the tgHD rats (8 months: WT, 11.9% ± 4% vs HD, 57.8% ± 16.5%; 12 months: WT, 15.9% ± 4.7% vs HD, 48.9% ± 22%). Thus, reduced neuronal differentiation of newly generated cells was associated with an increase of cells remaining undifferentiated and/or in a quiescent stem cell stage in the tgHD rats.

To define the cell identity of BrdU-positive undifferentiated cells in more detail, we determined the presence of Sox2, a marker for functional stem cell maintenance (38), and of the proliferation marker PCNA. There were more numerous Sox2-positive cells in tgHD than in WT DG (Fig. 3D), and the numbers of BrdU-positive/Sox2-positive cells were also significantly greater in the tgHD rats (Figs. 3F, G) (8 months: WT, 25% ± 1.6% vs HD, 52.5% ± 6.3%; 12 months, WT, 26.3% ± 9.7% vs HD, 61.62% ± 4%). In both genotypes, however, most of BrdU-retaining/Sox2-positive cells found in the subgranular zone (SGZ) were PCNA negative (Figs. 3E–G). Taken together, these data indicate that numbers of quiescent stem cells are increased in the tgHD hippocampus.

FIGURE 5. Enhanced transforming growth factor-β1 (TGF-β1)/Smad2 signaling in a transgenic rat model of Huntington disease (tgHD) rats. **(A)** The pSmad2 in 8-month-old wild-type (WT) dentate gyrus (DG) granule cells. The pSmad2 (green) was present in NeuN-positive (blue) cells and in mature doublecortin (DCX)-positive (red) cells. The DCX cells in the granule cell layer (GCL) presented a dendritic tree perpendicular to the subgranular zone (SGZ), whereas immature DCX-positive cells were in clusters with a less pronounced dendrite. Scale bars = 50 μm. Insets are higher magnifications of fields indicated by arrows. **(B)** The pSmad2 (green) was present in Sox2-positive (red) glial fibrillary acidic protein (GFAP)–positive (blue) cells in a 12-month-old tgHD SGZ (right panels), but not in a WT SGZ (left panels). Scale bars = 50 μm. Insets are higher magnifications of the selected fields. **(C)** Quantitative analysis of Sox2 and Sox2-positive/GFAP-positive cells that were pSmad2 positive in 12-month-old WT and tgHD. The pSmad2 colocalized to a greater extent in Sox2-positive cells (***$p < 0.0001$) and Sox2-positive/GFAP-positive cells (***$p < 0.0001$) in the tgHD than the WT DG. Data were expressed as mean ± SD; 1-way analysis of variance–Tukey post hoc for statistical analysis. n = 4 for WT and n = 8 for tgHD. **(D)** Western blot demonstrates greater levels of pSmad2 in tgHD than in WT hippocampi. Smad2 and actin were used as controls.

Neuroblast Proliferation Compensates Stem Cell Quiescence in tgHD DG

As a consequence of increased stem cell quiescence in tgHD SGZ (Figs. 3D–G), total cell proliferation would likely be diminished; however, in 8-month-old tgHD DG, the rate of cell proliferation was unaffected (Figs. 1B, C). To elucidate this apparent incongruity, we investigated the identity of DG proliferating cells in 8-month-old tgHD rats. At 24 hours after BrdU injection, BrdU-positive nuclei were predominantly found in cell clusters typically containing a minimum of 3 to 6 cells in the innermost region of the GCL and in the SGZ (Fig. 4A). The numbers of such BrdU cell clusters (i.e. "proliferating units") were significantly reduced in the tgHD DG versus WT rats (8 months: WT, 43.5 ± 13.3 vs HD, 23.2 ± 10.3; 12 months: WT, 15 ± 6 vs HD, 4.5 ± 2.7) (Fig. 4B). The numbers of BrdU-positive cells per unit and, as a consequence, the activity of the proliferating units were significantly greater in 8-month-old, but not in 12-month-old, tgHD rats (8 months: HD, cluster size 369.4 ± 166 μm^2, 6.6 ± 1.2 cells/cluster; WT, cluster size 115 ± 115 μm^2, 4.2 ± 1.2 cells/cluster) (Figs. 4C, D). Colabeling of BrdU-positive cells in the clusters with the neuroblast marker DCX revealed significantly greater proportions of DCX-positive cells in 8-month-old tgHD rats (WT, 47% ± 5% vs HD, 73% ± 6.6%) (Fig. 4E). This increase was also reflected in total numbers of DCX-positive cells, which expanded by 237.5% in the DG of tgHD versus WT rats (Figs. 4F, G). Moreover, DCX-positive axons projecting toward the CA3 regions were frequently and specifically observed in the hilus of 8-month-old tgHD rats (Fig. 4G). The total number of DCX-positive cells was significantly reduced by 58.7% in the DG of 12-month-old tgHD rats versus their WT littermates (Fig. 4F). This reduction most likely resulted from a combination of impaired proliferation and reduced survival (Figs. 1 and 2).

Thus, despite the elevated numbers of quiescent Sox2-positive stem cells, the overall proliferation level in the DG was maintained in the DG of 8-month-old tgHD rats through a compensatory increased proliferation of the DCX-positive neuroblast population. However, in 12-month-old tgHD rats, the marked proliferative and survival deficit could not be overcome.

Reduced Cell Proliferation in tgHD Rats Correlates With Increased TGF-β1 Signaling in Hippocampal Stem Cells

We and others have demonstrated that TGF-β1 impairs neural stem and progenitor cell proliferation (15, 18, 19). Moreover, we found that TGF-β1 mRNA expression and the TGF-β downstream effector elements Smad2 and Smad4 and the TGF-β–inducible extracellular matrix components are elevated in human HD brains (6). These data suggest a possible elevation of TGF-β signaling in tgHD hippocampus that might provide an explanation for the reduced stem cell proliferation. We therefore assessed TGF-β signaling in the DG by IHC for phospho-Smad2, an intracellular TGF-β downstream effector molecule (39).

Confocal analysis for pSmad2 immunoreactivity (IR) in the DG of WT rats revealed that pSmad2 staining was weak and confined almost exclusively to NeuN-positive cells in the GCL (Fig. 5A). In addition, DCX-positive cells with a mature morphology (i.e. with extensive dendritic arborization) were also pSmad2 positive, whereas DCX cells in the SGZ within clusters or displaying an immature morphology were pSmad2 negative (Fig. 5A). The GFAP-positive/Sox2-positive cells in the SGZ were virtually devoid of pSmad2 IR (Fig. 5B).

In contrast, in 8-month-old (not shown) and, to a greater degree, in 12-month-old tgHD rats, the global pSmad2 staining intensity was greater in cells of the GCL (Fig. 5B). Strikingly, overt pSmad2 IR was present in GFAP-positive/Sox2-positive cells of the SGZ at 8-month-old (not shown), and even stronger for 12-month-old tgHD rats (Fig. 5B). In addition to staining intensity, the numbers of Sox2-positive cells and of Sox2-positive/GFAP-positive cells in the SGZ

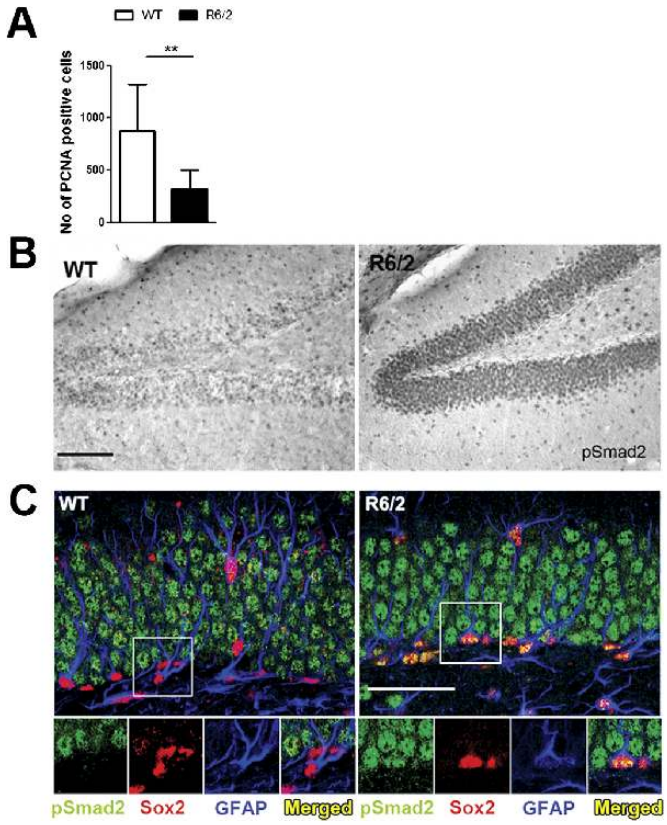

FIGURE 6. Reduced proliferation was associated with increased transforming growth factor-β1 (TGF-β1) signaling in R6/2 mice. **(A)** Quantitative analysis of proliferating cell nuclear antigen (PCNA)–positive cells in the dentate gyrus (DG) of 9-week-old wild-type (WT) and R6/2 mice. Data were expressed as mean ± SD. There were fewer PCNA-positive cells in R6/2 and WT DG (**$p < 0.001$) (Student *t*-test). **(B)** The pSmad2 immunoreactivity (IR) in WT and R6/2 DG. There was prominent pSmad2 IR in the R6/2 DG. Scale bars = 100 μm. **(C)** Colocalization of pSmad2 (green) IR in Sox2-positive (red)/glial fibrillary acidic protein (GFAP)-positive (blue) cells in the DG of WT and R6/2 mice. Scale bars = 100 μm. There was pSmad2 IR in Sox2-positive/GFAP-positive cells in R6/2 but not in WT mice. Boxed areas are shown at higher magnification in insets.

that colabeled for pSmad2 were significantly enhanced in the tgHD rats (Sox2/pSmad2: WT, 20% ± 2.2% vs HD, 56% ± 7.7%; Sox2/GFAP/pSmad2: WT, 18.5% ± 1.9% vs HD, 42.2% ± 8.7%) (Fig. 5C). Western blot analyses confirmed a global increase in Smad2 phosphorylation in the tgHD hippocampus (Fig. 5D).

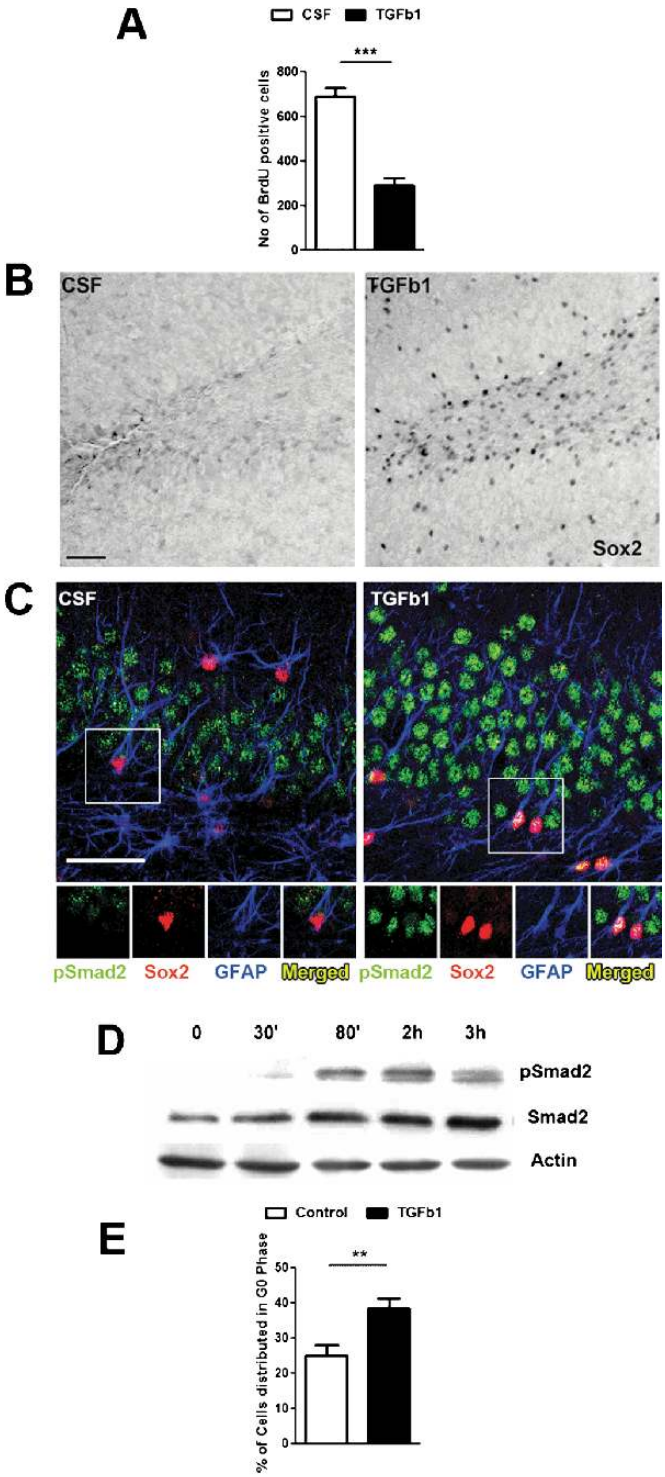

To substantiate these observations, we analyzed hippocampi of R6/2 mice, another well-characterized model for HD (2). At 9 weeks of age, cell proliferation in the R6/2 DG was significantly reduced, as demonstrated by a decrease in numbers of PCNA-positive cells (Fig. 6A, see also [12]). This correlated with greater levels of pSmad2 IR in the DG of R6/2 mice than in WT mice (Fig. 6B). Moreover, whereas there was virtually no pSmad2 labeling in GFAP-positive/Sox2-positive cells in the SGZ of WT mice, this putative stem cell population showed strong pSmad2 IR in R6/2 animals (Fig. 6C).

We next confirmed that elevated TGF-β in the brain per se was sufficient to provoke the appearance of pSmad2 in the hippocampal stem cell niche by infusing TGF-β1 into the lateral ventricle of WT rats for 14 days and analyzing cell proliferation and the pattern of pSmad2 staining in Sox2-positive cells. As previously reported (18, 19), TGF-β1 infusion induced strong inhibition of proliferation in the hippocampal DG (aCSF, 689 ± 40.6 BrdU-positive cells vs TGF-β1, 293 ± 31.8 BrdU-positive cells) (Fig. 7A). This proliferative decline was associated with an increase in the numbers of Sox2-positive cells (Fig. 7B). As in naive WT rats, pSmad2 was weakly but consistently present in cells of the GCL and absent in the Sox2-positive/GFAP-positive cells of aCSF-infused rats (Fig. 7C). In contrast, infusion of TGF-β1 in WT rats enhanced the staining intensity of pSmad2 in the GCL and induced the presence of pSmad2 in Sox2-positive/GFAP-positive SGZ cells with a similar pattern as observed in the tgHD rats (Fig. 7C). Moreover, TGF-β1 induced a fast appearance of pSmad2 in adult rat–derived neural progenitors in culture (Fig. 7D), indicating that these cells are responsive to TGF-β1.

Finally, we determined whether TGF-β1 provokes a cell cycle arrest in neural progenitors by stimulating neural progenitors derived from the adult rat hippocampus (19) in vitro with TGF-β1 and analyzing the cell cycle phases by Ki67/PI flow cytometry. This method allows the dissection of

FIGURE 7. Transforming growth factor-β1 (TGF-β1)–directed proliferation and cell cycle arrest were associated with enhanced SMAD2 signaling in the stem cell niche. **(A)** Numbers of 5-bromo-2-deoxyuridine (BrdU)–positive cells in the dentate gyrus (DG) of TGF-β1– and artificial cerebrospinal fluid (aCSF)–infused rats. Data were expressed as mean ± SD. There were fewer BrdU-positive cells in TGF-β1–infused than in control rats (***$p < 0.0001$) (Student *t*-test). **(B)** Sox2 immunoreactivity (IR) in the DG of aCSF- and TGF-β1–infused animals. There was prominent Sox2 IR in TGF-β1–infused DG. Scale bars = 50 μm. **(C)** Confocal analysis of Sox2-positive (red)/glial fibrillary acidic protein (GFAP)–positive (blue) cells with pSmad2 IR (green) in the DG of aCSF- and TGF-β1–infused animals. Scale bars = 50 μm. Insets are focused on the selected fields. There was prominent pSmad2 IR in the Sox2-positive/GFAP-positive subgranular zone (SGZ) cells in TGF-β1–infused but not aCSF-infused animals. **(D)** Western blot analysis demonstrating TGF-β1–induced phosphorylation of Smad2 in neural progenitor cultures. Smad2 and actin were used as controls. **(E)** Quantitative analysis of Ki67/PI flow cytometry of neural progenitors demonstrating TGF-β1–induced cell cycle phase shift into G_0 (**$p < 0.01$) (Student *t*-test).

G_0 and G_1 because Ki67 is expressed throughout the cell cycle except in G_0 (33). The analysis revealed that TGF-β1 treatment for 7 days induced a shift to G_0 phase of the cell cycle (G_0: control, 24.8% ± 3% vs TGF-β1, 38.5% ± 2.7%) (Fig. 7E). This indicates that TGF-β1 induces neural progenitors to exit the cell cycle and to become quiescent.

DISCUSSION

We demonstrate impaired progenitor proliferation associated with an increase in neural stem cell quiescence in animal models of HD (Fig. 8). Signaling of TGF-β1 seems to be involved in triggering quiescence of stem cells, as suggested by the presence of pSmad2 in Sox2-positive/GFAP-positive SGZ cells in tgHD rats, R6/2 mice, and after TGF-β infusion, and by the TGF-β1–induced cell cycle arrest in neural progenitor cultures. In 8-month-old tgHD rats (the early phase of the disease), the stem cell proliferation deficit was compensated by increased DCX-positive neuroblast proliferation, which resulted in an expansion of DCX-positive cells. Survival of newly generated cells, the total number of DG neurons, and neuronal density were also reduced in tgHD rats. These findings correlated with weaker pCREB signaling (Fig. 2), and similar observations were previously reported for R6/2 mice (9, 10, 12). Further evidence for reduced pCREB signaling in HD was provided by expression profiling of human HD brains demonstrating a downregulation of CREB-regulated transcription coactivator 1, of p300/CBP-associated factor, and of cyclic AMP-regulated phosphoprotein (6).

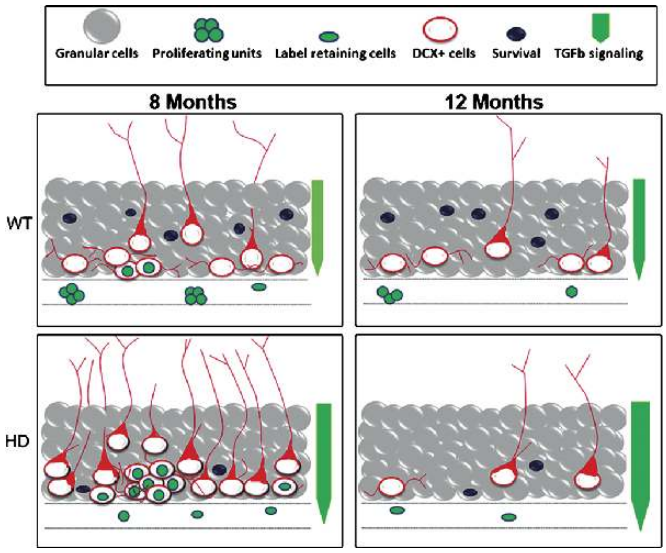

FIGURE 8. Schematic summary of modulation of neurogenesis at different cellular levels in the transgenic rat model of Huntington disease (tgHD). In 8-month-old tgHD animals, the deficit in stem/progenitor proliferation was compensated by doublecortin (DCX)-positive neuroblasts (red cells) resulting in an overall increase in the DCX population. In 12-month-old tgHD rats, reduced proliferation of progenitors was accompanied by a reduced number of DCX-positive cells. There were fewer surviving newly generated cells (round-shaped dark blue cells) in 8- and 12-month-old tgHD than in wild-type (WT) animals. The numbers of label-retaining quiescent subgranular zone stem cells, however, were elevated in tgHD animals. In WT, transforming growth factor-β1 (TGF-β1) signaling (fluorescence green arrow) was confined to cells of granule cell layer (gray cells) and it was absent or low in the stem cell niche. In tgHD animals, however, the overall TGF-β1 signaling was greater and prominent in the stem cell niche where it induced cell cycle exit and stem cell quiescence.

Neural Stem Cell Quiescence in Neurodegeneration

One of the most striking findings of this study is the disease-associated quiescence of neural stem cells in the hippocampal stem cell niche. This quiescence was revealed by an expansion in the pool of label-retaining nonproliferative and undifferentiated cells that additionally expressed the stem cell maintenance marker Sox2. Several studies have also reported reduced progenitor proliferation rates in animal models of neurodegeneration. This proliferative decline was documented in the R6/1 and R6/2 HD mouse models (9–14, 40, 41), in the A53T mutant α-synuclein Parkinson disease mouse model (42), in a mouse model of Alzheimer disease in which there is expression of the human amyloid precursor protein with the V717F mutation (43), and in the superoxide dismutase 1 mouse model of amyotrophic lateral sclerosis (44). Reduced neurogenesis in chronic neurodegenerative disease cannot be taken as a general phenomenon, however, because cell proliferation in the subventricular zone of HD brains and hippocampal neurogenesis in AD brains are enhanced (45, 46).

A reduction in the numbers of proliferating cells might result from 1) lower numbers of proliferation-competent stem/progenitor cells, 2) slower proliferation rate (i.e. a prolonged cell cycle), or 3) a shift of stem cells from the proliferative status to quiescence. Our present findings strongly support the latter hypothesis, although a participation of the other mechanisms cannot be excluded. It is now crucial to determine whether TGF-β remodeling of the stem cell niche and induction of stem cell quiescence during the course of neurodegeneration is a widespread phenomenon or restricted to a subtype of conditions such as HD.

Under physiological conditions, stem cells may limit their mitotic activity and remain mostly in quiescence (G_0) until a self-renewing cycle is required to maintain a steady state pool and prevent depletion of the stem cell pool. On one hand, acute CNS lesions (e.g. stroke and quinolinic acid– or 6-hydroxydopamine–induced striatal lesions) apparently provide a stimulus to foster stem and progenitor cell proliferation, which is probably an attempt to compensate for the neuronal loss (47–49). On the other hand, slow progressive neurodegeneration often compromises progenitors in their proliferative activity. Whether this inhibitory response serves a specific function or is a negative side effect deriving from a disease-associated microenvironmental change such as inflammatory responses remains to be determined. Enhanced neural stem cell quiescence, however, might be a mechanism for maintaining or preserving the stem cell pool. Indeed, the potential to generate neurospheres from the R6/2 mouse is higher than that of WT animals (50), and neural progenitors derived from HD mice demonstrate increased neuronal differentiation (51).

TGF-β1 Signaling as a Potential Mechanism Triggering Stem Cell Quiescence in Neurodegeneration

Inflammatory processes are involved in many acute and chronic neurodegenerative conditions, and a plethora of anti-inflammatory and proinflammatory cytokines, chemokines, neurotransmitters, and reactive oxygen species is released (52). The specific pattern of inflammatory cells and cytokines in the neural stem cell niche under pathological conditions might modulate the molecular and cellular context of TGF-β action and thereby might create apparently divergent TGF-β–associated effects (53). One example for this cellular context–dependent Janus head–like activity of TGF-β is the fact that TGF-β acts for most cells as an antimitotic cytokine, whereas it promotes tumor cell proliferation (15). This context dependency might also explain conflicting data on enhanced cell proliferation in the subventricular zone in HD (54) and diminished progenitor proliferation in the hippocampal neurogenic niche in HD animal models (9–14, 40, 41). Our present data indicate that differences in cellular responses can be documented between the putative stem cell and the neuronal progenitors.

Although the pathways induced by TGF-β leading to neural stem cell quiescence require further molecular investigation, mechanisms are likely to be similar to those previously described in other systems, particularly the hematopoietic system. In the latter, Pbx1 and Pbx1-dependent genes and FoxO3 may be effectors of TGF-β–induced quiescence (55, 56). FoxO3 is a central stem cell maintenance factor integrating a plethora of signaling cascades including the interleukin-2R/signal transducers and activators of transcription pathway, the TGF-β/Smad pathway, the phosphoinositide-3 kinase/Akt/mammalian target of rapamycin cascade, and Notch signaling, and is, therefore, likely involved in the signaling leading to neural stem cell quiescence (57).

The Possible Impact of Huntingtin Transgene Expression on Neural Stems in tgHD Rats

In addition to the microenvironment-induced effects on neural stem cell proliferation, the expression of the huntingtin transgene in our animal models might exert cell-intrinsic activities that contribute to the cell cycle exit and quiescence. A prerequisite for this, however, would be that the huntingtin transgene is indeed expressed in neural stem cells. We performed IHC for endogenous and/or transgenic huntingtin using the IC2 and EM48 antibodies in the tgHD rats but could not detect any immunoreactivity in the hippocampal neural stem cell niche (data not shown). Previously, however, we demonstrated increasing expression of the huntingtin protein between 9 and 15 months of age, specifically in mature neurons (4). Our analysis of R6/2 mice also revealed that mutant huntingtin was only present in mature hippocampal granule cells and not in neuronal precursors or neural stem cells (12). Thus, interference with the neuronal maturation process by the mutant and aggregated huntingtin could explain diminished survival of newly generated neurons. We cannot exclude the possibility that the presence of minute amounts of huntingtin protein negatively affects neural stem cell proliferation, but the main mechanism by which neurogenesis is reduced in HD models seems to be via a remodeling of the stem cell niche microenvironment.

In conclusion, we report that neurogenesis in the tgHD rat hippocampus is impaired via mechanisms acting at different levels along the generation of new mature neurons. Our evidence supports the hypothesis that defects in progenitor proliferation and cell cycle exit are orchestrated by TGF-β signaling in the local microenvironment.

ACKNOWLEDGMENTS

The authors thank Robert Aigner, Massimiliano Caioni, Katrin Stadler, and Sonja Plötz for excellent technical support.

REFERENCES

1. The Huntington's Disease Collaborative Research Group. A novel gene containing a trinucleotide repeat that is expanded and unstable on Huntington's disease chromosomes. Cell 1993;72:971–83
2. Mangiarini L, Sathasivam K, Seller M, et al. Exon 1 of the HD gene with an expanded CAG repeat is sufficient to cause a progressive neurological phenotype in transgenic mice. Cell 1996;87:493–506
3. von Horsten S, Schmitt I, Nguyen HP, et al. Transgenic rat model of Huntington's disease. Hum Mol Genet 2003;12:617–24
4. Nguyen HP, Kobbe P, Rahne H, et al. Behavioral abnormalities precede neuropathological markers in rats transgenic for Huntington's disease. Hum Mol Genet 2006;15:3177–94
5. Petrasch-Parwez E, Nguyen HP, Lobbecke-Schumacher M, et al. Cellular and subcellular localization of Huntingtin [corrected] aggregates in the brain of a rat transgenic for Huntington disease. J Comp Neurol 2007; 501:716–30
6. Bode FJ, Stephan M, Suhling H, et al. Sex differences in a transgenic rat model of Huntington's disease: Decreased 17β-estradiol levels correlate with reduced numbers of DARPP32+ neurons in males. Hum Mol Genet 2008;17:2595–609
7. Gellerich FN, Gizatullina Z, Nguyen HP, et al. Impaired regulation of brain mitochondria by extramitochondrial Ca2+ in transgenic Huntington disease rats. J Biol Chem 2008;283:30715–24
8. Ming GL, Song H. Adult neurogenesis in the mammalian central nervous system. Annu Rev Neurosci 2005;28:223–50
9. Lazic SE, Grote H, Armstrong RJ, et al. Decreased hippocampal cell proliferation in R6/1 Huntington's mice. Neuroreport 2004;15:811–13
10. Gil JM, Mohapel P, Araujo IM, et al. Reduced hippocampal neurogenesis in R6/2 transgenic Huntington's disease mice. Neurobiol Dis 2005;20: 744–51
11. Lazic SE, Grote HE, Blakemore C, et al. Neurogenesis in the R6/1 transgenic mouse model of Huntington's disease: Effects of environmental enrichment. Eur J Neurosci 2006;23:1829–38
12. Kohl Z, Kandasamy M, Winner B, et al. Physical activity fails to rescue hippocampal neurogenesis deficits in the R6/2 mouse model of Huntington's disease. Brain Res 2007;1155:24–33
13. Duan W, Peng Q, Masuda N, et al. Sertraline slows disease progression and increases neurogenesis in N171-82Q mouse model of Huntington's disease. Neurobiol Dis 2008;30:312–22
14. Peng Q, Masuda N, Jiang M, et al. The antidepressant sertraline improves the phenotype, promotes neurogenesis and increases BDNF levels in the R6/2 Huntington's disease mouse model. Exp Neurol 2008;210: 154–63
15. Aigner L, Bogdahn U. TGF-β in neural stem cells and in tumors of the central nervous system. Cell Tissue Res 2008;331:225–41
16. Ilzecka J, Stelmasiak Z, Dobosz B. Transforming growth factor-β1 (TGF-β1) in patients with amyotrophic lateral sclerosis. Cytokine 2002; 20:239–43
17. Jason GW, Suchowersky O, Pajurkova EM, et al. Cognitive manifestations of Huntington disease in relation to genetic structure and clinical onset. Arch Neurol 1997;54:1081–88
18. Buckwalter MS, Yamane M, Coleman BS, et al. Chronically increased transforming growth factor-β1 strongly inhibits hippocampal neurogenesis in aged mice. Am J Pathol 2006;169:154–64

19. Wachs FP, Winner B, Couillard-Despres S, et al. Transforming growth factor-β1 is a negative modulator of adult neurogenesis. J Neuropathol Exp Neurol 2006;65:358–70
20. Bizon JL, Lee HJ, Gallagher M. Neurogenesis in a rat model of age-related cognitive decline. Aging Cell 2004;3:227–34
21. Clelland CD, Choi M, Romberg C, et al. A functional role for adult hippocampal neurogenesis in spatial pattern separation. Science 2009;325:210–13
22. Hernandez-Rabaza V, Llorens-Martin M, Velazquez-Sanchez C, et al. Inhibition of adult hippocampal neurogenesis disrupts contextual learning but spares spatial working memory, long-term conditional rule retention and spatial reversal. Neuroscience 2009;159:59–68
23. Jessberger S, Clark RE, Broadbent NJ, et al. Dentate gyrus–specific knockdown of adult neurogenesis impairs spatial and object recognition memory in adult rats. Learn Mem 2009;16:147–54
24. Tada T. Disturbed spatial learning of rats after intraventricular administration of transforming growth factor-β1. Neurol Med Chir (Tokyo) 2002;42:151–56 [discussion 7]
25. Wyss-Coray T, Feng L, Masliah E, et al. Increased central nervous system production of extracellular matrix components and development of hydrocephalus in transgenic mice overexpressing transforming growth factor-β1. Am J Pathol 1995;147:53–67
26. Wyss-Coray T, Lin C, Sanan DA, et al. Chronic overproduction of transforming growth factor-β1 by astrocytes promotes Alzheimer's disease–like microvascular degeneration in transgenic mice. Am J Pathol 2000;156:139–50
27. Wyss-Coray T, Lin C, Yan F, et al. TGF-β1 promotes microglial amyloid-β clearance and reduces plaque burden in transgenic mice. Nat Med 2001;7:612–88
28. Couillard-Despres S, Winner B, et al. Doublecortin expression levels in adult brain reflect neurogenesis. Eur J Neurosci 2005;21:1–14
29. Gundersen HJ, Bagger P, Bendtsen TF, et al. The new stereological tools: Dissector, fractionator, nucleator and point sampled intercepts and their use in pathological research and diagnostics. APMIS 1988;96:857–81
30. Williams RW, Rakic P. Three-dimensional counting: An accurate and direct method to estimate numbers of cells in sectioned material. J Comp Neurol 1988;278:344–52
31. Seki T, Namba T, Mochizuki H, et al. Clustering, migration, and neurite formation of neural precursor cells in the adult rat hippocampus. J Comp Neurol 2007;502:275–90
32. Wachs FP, Couillard-Despres S, Engelhardt M, et al. High efficacy of clonal growth and expansion of adult neural stem cells. Lab Invest 2003;83:949–62
33. Endl E, Steinbach P, Knuchel R, et al. Analysis of cell cycle–related Ki-67 and p120 expression by flow cytometric BrdUrd-Hoechst/7AAD and immunolabeling technique. Cytometry 1997;29:233–41
34. Van Raamsdonk JM, Pearson J, Rogers DA, et al. Loss of wild-type huntingtin influences motor dysfunction and survival in the YAC128 mouse model of Huntington disease. Hum Mol Genet 2005;14:1379–92
35. Ciamei A, Morton AJ. Rigidity in social and emotional memory in the R6/2 mouse model of Huntington's disease. Neurobiol Learn Mem 2008;89:533–44
36. Jagasia R, Steib K, Englberger E, et al. GABA-cAMP response element-binding protein signalling regulates maturation and survival of newly generated neurons in the adult hippocampus. J Neurosci 2009;29:7966–77
37. Walton M, Woodgate AM, Muravlev A, et al. CREB phosphorylation promotes nerve cell survival. J Neurochem 1999;73:1836–42
38. Graham V, Khudyakov J, Ellis P, et al. SOX2 functions to maintain neural progenitor identity. Neuron 2003;39:749–65
39. Massague J. TGF-β signal transduction. Annu Rev Biochem 1998;67:753–91
40. Grote HE, Bull ND, Howard ML, et al. Cognitive disorders and neurogenesis deficits in Huntington's disease mice are rescued by fluoxetine. Eur J Neurosci 2005;22:2081–88
41. Phillips W, Morton AJ, Barker RA. Abnormalities of neurogenesis in the R6/2 mouse model of Huntington's disease are attributable to the in vivo microenvironment. J Neurosci 2005;25:11564–76
42. Winner B, Rockenstein E, Lie DC, et al. Mutant alpha-synuclein exacerbates age-related decrease of neurogenesis. Neurobiol Aging 2008;29:913–25
43. Donovan MH, Yazdani U, Norris RD, et al. Decreased adult hippocampal neurogenesis in the PDAPP mouse model of Alzheimer's disease. J Comp Neurol 2006;495:70–83
44. Liu Z, Martin LJ. The adult neural stem and progenitor cell niche is altered in amyotrophic lateral sclerosis mouse brain. J Comp Neurol 2006;497:468–88
45. Curtis MA, Penney EB, Pearson AG, et al. Increased cell proliferation and neurogenesis in the adult human Huntington's disease brain. Proc Natl Acad Sci U S A 2003;100:9023–27
46. Jin K, Peel AL, Mao XO, et al. Increased hippocampal neurogenesis in Alzheimer's disease. Proc Natl Acad Sci U S A 2004;101:343–47
47. Kokaia Z, Thored P, Arvidsson A, et al. Regulation of stroke-induced neurogenesis in adult brain—recent scientific progress. Cereb Cortex 2006;16(Suppl 1):i162–67
48. Tattersfield AS, Croon RJ, Liu YW, et al. Neurogenesis in the striatum of the quinolinic acid lesion model of Huntington's disease. Neuroscience 2004;127:319–32
49. Winner B, Couillard-Despres S, Geyer M, et al. Dopaminergic lesion enhances growth factor–induced striatal neuroblast migration. J Neuropathol Exp Neurol 2008;67:105–16
50. Batista CM, Kippin TE, Willaime-Morawek S, et al. A progressive and cell non-autonomous increase in striatal neural stem cells in the Huntington's disease R6/2 mouse. J Neurosci 2006;26:10452–60
51. Lorincz MT, Zawistowski VA. Expanded CAG repeats in the murine Huntington's disease gene increases neuronal differentiation of embryonic and neural stem cells. Mol Cell Neurosci 2009;40:1–13
52. Das S, Basu A. Inflammation: A new candidate in modulating adult neurogenesis. J Neurosci Res 2008;86:1199–208
53. Whitney NP, Eidem TM, Peng H, et al. Inflammation mediates varying effects in neurogenesis: Relevance to the pathogenesis of brain injury and neurodegenerative disorders. J Neurochem 2009;108:1343–59
54. Curtis MA, Connor B, Faull RL. Neurogenesis in the diseased adult human brain—new therapeutic strategies for neurodegenerative diseases. Cell Cycle 2003;2:428–30
55. Chabanon A, Desterke C, Rodenburger E, et al. A cross-talk between stromal cell–derived factor-1 and transforming growth factor-β controls the quiescence/cycling switch of CD34(+) progenitors through FoxO3 and mammalian target of rapamycin. Stem Cells 2008;26:3150–61
56. Ficara F, Murphy MJ, Lin M, et al. Pbx1 regulates self-renewal of long-term hematopoietic stem cells by maintaining their quiescence. Cell Stem Cell 2008;2:484–96
57. Shen Z, Chen L, Hao F, et al. Transcriptional regulation of Foxp3 gene: Multiple signal pathways on the road. Med Res Rev 2009;29:742–66